ACS OMEGA

http://pubs.acs.org/journal/acsodf

Article

Simple Regulation of the Self-Assembling Ability by Multimerization of Elastin-Derived Peptide $(FPGVG)_n$ Using Nitrilotriacetic Acid as a Building Block

Keitaro Suyama, Mika Mawatari, Daiki Tatsubo, Iori Maeda, and Takeru Nose*

Cite This: *ACS Omega* 2021, 6, 5705−5716

Read Online

ACCESS | Metrics & More | Article Recommendations | Supporting Information

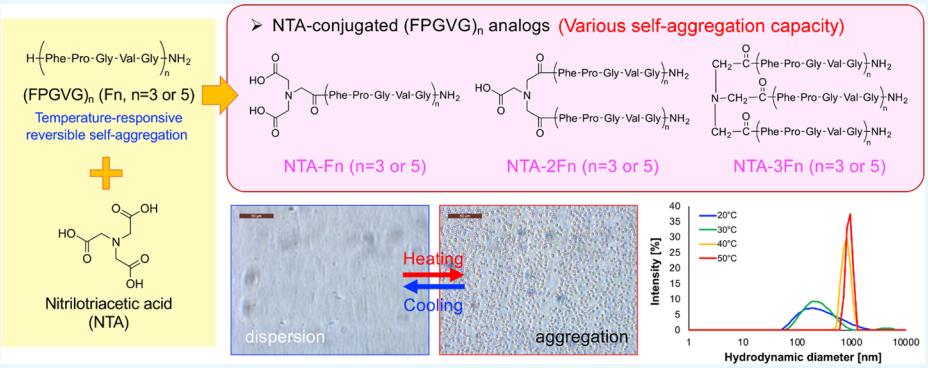

ABSTRACT: Elastin comprises hydrophobic repetitive sequences, such as Val-Pro-Gly-Val-Gly, which are thought to be important for the temperature-dependent reversible self-association (coacervation). Elastin and elastin-like peptides (ELPs), owing to their characteristics, are expected to be applied as base materials for the development of new molecular tools, such as drug-delivery system carrier and metal-scavenging agents. Recently, several studies have been reported on the dendritic or branching ELP analogues. Although the topological difference of the branched ELPs compared to their linear counterparts may lead to useful properties in biomaterials, the available information regarding the effect of branching on molecular architecture and thermoresponsive behavior of ELPs is scarce. To obtain further insight into the thermoresponsive behavior of branched ELPs, novel ELPs, such as nitrilotriacetic acid (NTA)−$(FPGVG)_n$ conjugates, that is, (NTA)-Fn analogues possessing 1−3 $(FPGVG)_n$ (n = 3, 5) molecule(s), were synthesized and investigated for their coacervation ability. Turbidity measurement of the synthesized peptide analogues revealed that (NTA)-Fn analogues showed strong coacervation ability with various strengths. The transition temperature of NTA-Fn analogues exponentially decreased with increasing number of residues. In the circular dichroism measurements, trimerization did not alter the secondary structure of each peptide chain of the NTA-Fn analogue. In addition, it was also revealed that the NTA-Fn analogue possesses one peptide chain that could be utilized as metal-scavenging agents. The study findings indicated that multimerization of short ELPs via NTA is a useful and powerful strategy to obtain thermoresponsive molecules.

1. INTRODUCTION

Thermoresponsive biomaterials are a class of materials that can modify their structures and properties in response to temperature change.[1] Over the last decade, interest in these materials has increased owing to their various potential applications as drug-delivery systems (DDS),[2−6] metal scavengers,[7,8] and protein separation supports.[9−11] Elastin-like peptides (ELPs), artificial peptides derived from elastin, belong to the class of thermoresponsive biomaterials whose properties have been widely explored. Elastin is a core protein of the elastic fibers and exists in the connective tissues, such as blood vessels, lungs, ligaments, and skin.[12] Tropoelastin, the precursor protein of elastin, exhibits a temperature-dependent reversible association/dissociation property, known as coacervation, which results in a phase transition with lower critical solution temperature (LCST) behavior under physiological conditions. This process has been considered to play an important role in the biosynthesis and elasticity of elastin.[13] Tropoelastin contains unique hydrophobic repeating sequences comprising consecutive three to six amino acid residues, such as Val-Pro-Gly-Val-Gly (VPGVG), Gly-Gly-Val-Pro (GGVP), and Gly-Val-Gly-Val-Ala-Pro (GVGVAP), in its hydrophobic domains.[12] These repetitive sequences are important for the coacervation of elastin

Received: December 16, 2020
Accepted: February 10, 2021
Published: February 18, 2021

and tropoelastin. ELPs also bearing these repetitive sequences exhibit the coacervation property and have been expected to be useful thermoresponsive materials. Among the different sequences, the pentapeptide sequence VPGVG is the most commonly identified repeating motif in mammalian species[14−16] and apparently exhibits coacervation.[13,17,18] Therefore, by mimicking such repetitive sequences, various ELP analogues composed of Xaa-Pro-Gly-Val-Gly (XPGVG) pentapeptide repeats have been developed.[19−24]

Extensive development of ELP-based biomaterials necessitates elucidation of the detailed mechanism of coacervation. Several intrinsic and extrinsic factors have been reported to influence the coacervation of ELPs. The coacervation ability of ELPs is primarily affected by the amino acid sequence and the number of hydrophobic amino acids present.[25] For example, an increment of the molecular weight, i.e., the number of peptide-repeats typically caused the transition temperature of ELPs to decrease.[26−28] Similarly, the characteristics of the peptide sequence also have a marked effect on the coacervation ability. For $(VPGVG)_n$, which is derived from a natural amino acid sequence of tropoelastin and is one of the benchmarks of ELPs, a sufficiently high repetition number ($n > 40$) is required to exhibit the coacervation ability.[19,29−31] However, substitution with a guest residue (X in VPGXG repetitive sequences, other than proline) altered the transition temperature (T_t) of ELPs.[27,32] That is, hydrophobic guest residues tend to decrease T_t, while hydrophilic guest residues elevate it. Previously, it has been reported that $(FPGVG)_n$ containing Phe instead of Val as hydrophobic aromatic amino acid residues shows potent coacervation ability at a significantly low number of repetition ($n = 5$).[20] These results clearly suggested that the hydrophobicity of the peptide holds significant importance in determining the coacervation ability.[19,20] Additional factors that influence the coacervation property of ELPs include the concentration of ELP, solution pH, and ionic strength. However, as most of these results were obtained from experiments using ELPs consisting of a single linear peptide chain, little is known about the effect of molecular architecture on the thermoresponsive behavior of ELPs.

Recently, several researchers have reported the study of dendritic ELP analogues[33−37] and ELPs in combination with branched polymer architectures, such as polyamidoamine (PAMAM).[38−41] Dendritic, hyperbranched, star, and other highly branched structures are important in biomaterials owing to their ability to be used in cross-linking structures to make polymeric hydrogels.[42] The nonlinear ELPs differ from the linear ones in terms of physical properties, such as solubility, viscosity, and resistance to proteolysis.[35,36,43] The topological differences in branched ELPs compared to their linear counterparts may lead to useful properties in biomaterials. However, the available information about the branching effect on molecular architecture and the thermoresponsive behavior of ELPs is scarce. Therefore, fundamental studies evaluating the effect of branching on thermoresponsive transitions of ELPs have been conducted to enable the design of new thermoresponsive materials with transitions in peptide secondary structure and solubility. Indeed, the multimerization techniques have recently become popular as a method to control the characteristics of ELPs including the stimuli responsiveness to pH, temperature, and light.[35−38,44−47] For example, ELP dendrimers with highly branched structures using lysine residues were synthesized and evaluated for their coacervation properties.[35,36] In this context, we previously reported that dimerized analogues of $(FPGVG)_5$ exhibit coacervation at a significantly lower temperature and concentration than their linear form $(FPGVG)_5$.[22] At present, the main driving force behind coacervation of ELPs is thought to be intermolecular hydrophobic interactions between the peptide molecules.[28] It was considered that this enhancement of the self-assembling ability of the dimerized peptides was due to the preferential formation of hydrophobic interactions between the peptide chains that were connected by dimerization. As (FPGVG)-based short ELP analogues exhibited strong coacervation ability in dimerization, it was considered that the multimerization of short-chain ELPs, which can be obtained by a simple chemical synthesis and purification procedure, could be an efficient method for accessing thermoresponsive molecules with self-assembling ability equivalent to that of long-chain ELPs. In comparison to short-chain ELPs, the chemical synthesis of long-chain ELPs is time- and resource-consuming. Thus, long ELPs cannot generally be synthesized by chemical synthesis but must be obtained as recombinant materials with synthetic genes. As the construction of protein expression systems is generally more expensive than the synthesis of simple short peptides, the multimerization of short 5-residue ELPs may be a more advantageous method of preparing temperature-responsive materials. Hence, additional studies are required to investigate the effect of further oligomerization and multimerization on coacervation of ELPs to control the self-assembly property of ELPs as novel biomaterials.

In this study, nitrilotriacetic acid (NTA) was selected as a central component of multimerization. As NTA has a symmetric structure and three carboxyl groups, we hypothesized that using this molecule would have the advantage of simultaneously obtaining the monomeric, dimeric, and trimeric conjugated analogues by condensing the *N*-terminus of the ELPs. In addition, NTA and their analogues are synthetic amino-polycarboxylic acids (APCA) that have been widely used as industrial chelating agents and are present as additives in many consumer products.[48] Therefore, some of the ELP analogues synthesized in this study could be used as basic materials for metal-scavenging agents. ELPs have been developed as effective absorbents for heavy metal removal and detection,[7,8,49−51] as ELPs with fused metal-binding domains can be readily produced and selectively tailored based upon the target metals. We hypothesized that the molecular structure of NTA, which is a building block for ELP multimerization, can be utilized as a metal-binding domain.

This study provides further insights into the contribution of multimerization of ELPs on coacervation. Novel monomer, dimer, and trimer ELP analogues that connected one to three H-$(FPGVG)_n$-NH_2 ($n = 3$, 5: F3 or F5) chains via NTA, namely, NTA-Fn, NTA-2Fn, and NTA-3Fn analogues, were synthesized and evaluated using a coacervation assay. In addition, temperature-dependent changes on the secondary structures of NTA-3F3 were investigated by circular dichroism (CD) spectroscopy to analyze the effect of trimerization on the secondary structure of the peptide. The temperature-dependent self-assembly of NTA-3F3 was also confirmed by particle size distribution measurement. Furthermore, the microscopic studies of the NTA-Fn analogue aggregates were carried out to obtain information on the morphology of the ELP aggregates. In addition, the metal-binding properties of NTA-3F3 were determined by colorimetric analysis and inductively coupled plasma mass spectroscopy (ICP-MS) to evaluate whether it can be used as a potential metal-scavenging agent.

https://dx.doi.org/10.1021/acsomega.0c06140
ACS Omega 2021, 6, 5705−5716

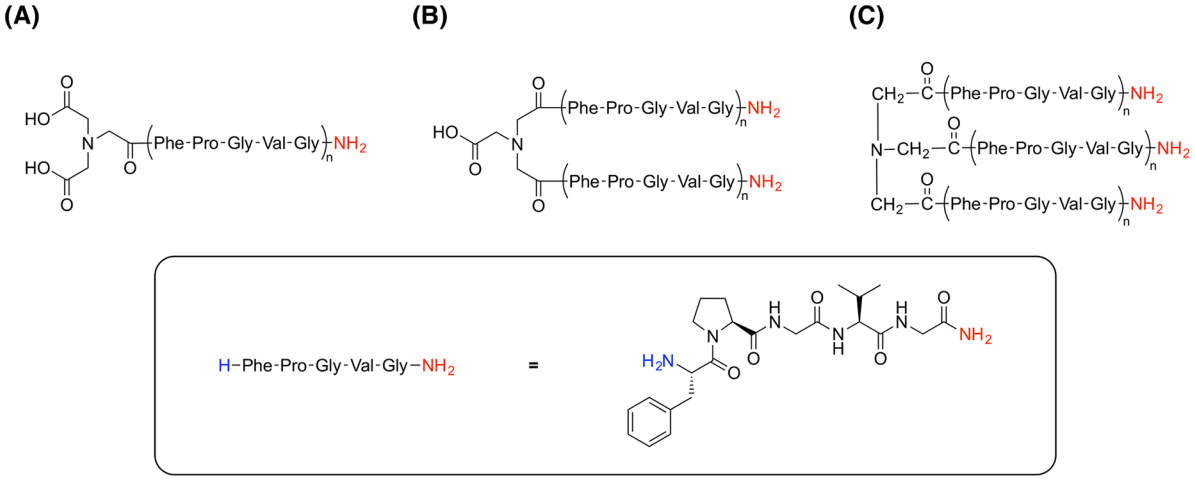

Figure 1. Chemical structures of NTA-Fn analogues. The chemical structures of (A) NTA-Fn, (B) NTA-2Fn, and (C) NTA-3Fn (n = 3 or 5) are shown. The *C*-terminus of each peptide was capped as an amide to avoid side reactions (represented using red letters).

Table 1. NTA-Fn Analogues Obtained in This Study

			MS (ESI) m/z		
peptide	yield (%)	retention time (min)[a]	composition formula	calculated	found
NTA-F3	35.3	2.069	$C_{75}H_{103}N_{17}O_{20}$	782.37 $[M + 2H]^{2+}$	782.37
NTA-2F3	11.0	3.352	$C_{144}H_{197}N_{33}O_{34}$	979.13 $[M + 3H]^{3+}$	979.29
NTA-3F3	16.0	3.816	$C_{213}H_{291}N_{49}O_{48}$	1077.50 $[M + 4H]^{4+}$	1077.70
NTA-F5	25.7	2.992	$C_{121}H_{165}N_{27}O_{30}$	1239.90 $[M + 2H]^{2+}$	1239.75
NTA-2F5	33.0	3.997	$C_{236}H_{321}N_{53}O_{54}$	1192.13 $[M + 4H]^{4+}$	1192.25
NTA-3F5	20.8	4.420	$C_{351}H_{477}N_{79}O_{78}$	1176.20 $[M + 6H]^{6+}$	1176.20

[a]Retention times of each peptide were determined by reversed phase-ultra performance liquid chromatography-tandem mass spectrometry (RP-UPLC-MS).

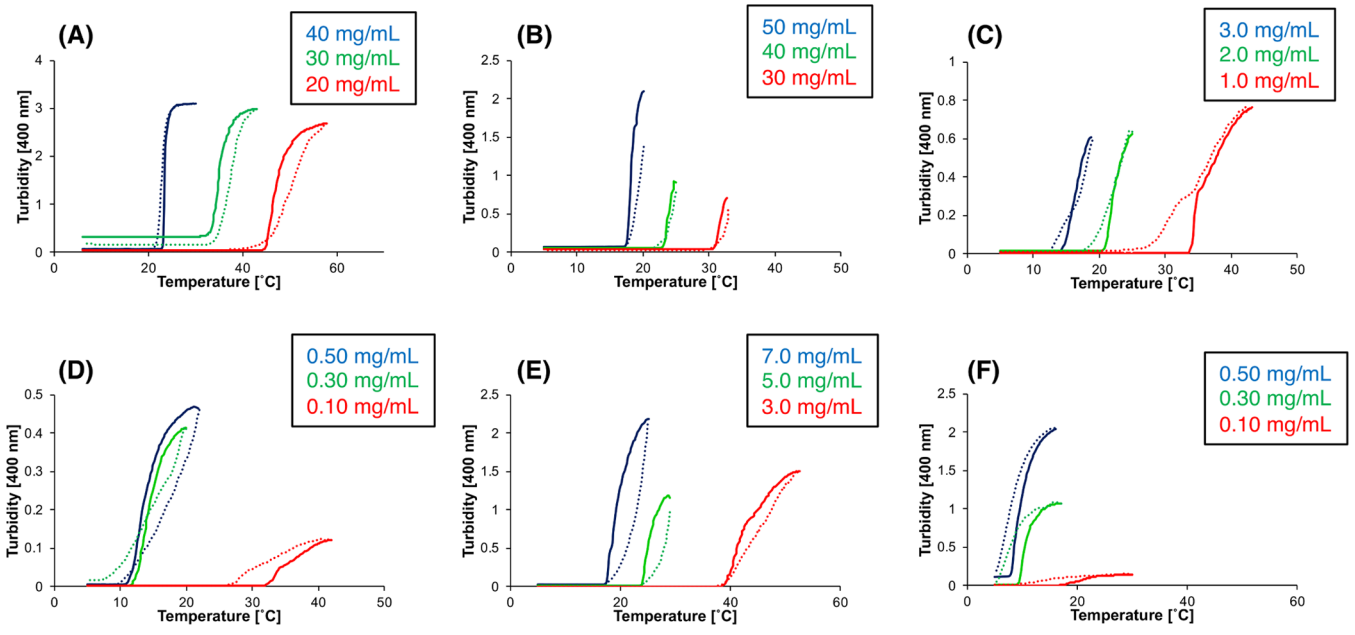

Figure 2. Turbidity profiles of NTA-Fn analogues at each concentration. Turbidity changes of (A) F5 (20−40 mg/mL), (B) NTA-F3 (30−50 mg/mL), (C) NTA-2F3 (1.0−3.0 mg/mL), (D) NTA-3F3 (0.10−0.30 mg/mL), (E) NTA-F5 (3.0−7.0 mg/mL), and (F) NTA-2F5 (0.10−0.50 mg/mL) associated with heating (solid lines) and cooling (dashed lines). NTA-3F5 was not dissolved in water at even 0.1 mg/mL concentration.

2. RESULTS AND DISCUSSION

2.1. Synthesis and Purification of Peptides. Elastin-derived peptide analogues H-$(FPGVG)_n$-NH_2 (n = 3, 5), F3 and F5, were successfully synthesized by the conventional solid-phase peptide synthesis procedure. To avoid undesired side reactions, the *C*-terminus of each peptide was capped as an amide group. Then, the NTA-Fn analogues were synthesized by conjugation of the *N*-terminal amino group on $(FPGVG)_n$ to

https://dx.doi.org/10.1021/acsomega.0c06140
ACS Omega 2021, 6, 5705−5716

one of the carboxy groups on an NTA molecule using 1-ethyl-3-(3-dimethylaminopropyl) carbodiimide monohydrochloride (WSCD) as the condensing agent. The molecular structures of the synthesized peptides are shown in Figure 1. In this reaction, NTA was used without capping any of the carboxyl groups to obtain NTA-Fn, NTA-2Fn, and NTA-3Fn as a mixture. Consequently, NTA-Fn and NTA-2Fn were obtained as a mixture and separated by high performance liquid chromatography (HPLC). However, NTA-3Fn, which contains three peptide chains, was not obtained utilizing WSCD as the condensing agent. It was anticipated that the steric hindrance around the reaction point on the dimeric NTA-2Fn interferes with the condensation of one more $(FPGVG)_n$ peptide. Therefore, the trimeric analogues were synthesized using (1-cyano-2-ethoxy-3 oxoethylidenaminooxy) dimethylamino-morpholino-carbenium hexafluoro phosphate (COMU), which is a more sophisticated and powerful condensing agent than WSCD. Ultra performance liquid chromatography-tandem mass spectrometry (UPLC-MS) revealed that the conjugation reaction of NTA to Fn proceeded progressively through NTA-Fn, NTA-2Fn, and NTA-3Fn. The purity and molecular weight of the synthesized peptides were also confirmed by UPLC-MS (Table 1). Results indicated the NTA-Fn analogues to be of high purity (Figure S1). The NTA-Fn analogues were readily synthesized compared to the corresponding linear peptides containing the same number of amino acid residues.

2.2. Turbidity Measurement. The temperature-dependent coacervation properties of the synthetic peptides were evaluated by measuring the turbidity of the aqueous peptide solutions at various concentrations (Figure 2 and Table 2). To quantitatively evaluate the coacervation properties of ELPs, T_t was calculated from the change in turbidity. The concentration range of the peptide solution was adjusted depending upon the water solubility of each peptide. First, turbidity measurements of monomeric ELP analogues (F3 and F5) were carried out. In this study, F3 showed no coacervation at 20−50 mg/mL (Figure S2). F5 required a concentration of at least 20 mg/mL to exhibit coacervation (Figure 2A). On the other hand, NTA-conjugates NTA-F3 and NTA-F5 showed relatively lower T_t at low concentration than F3 and F5, respectively (Figure 2B,D). These findings indicated that the coacervation ability of the NTA-conjugates was enhanced. Enhancement was considered to be a result of increased hydrophobicity of NTA-conjugated F3 and F5. In the coacervation measurement, the aqueous solution of ELPs was acidic (approximately pH 2.4−2.6) due to the small amount of remaining trifluoroacetic acid (TFA) in the solution derived from the HPLC-purification of peptides. Therefore, it was considered that the carboxyl groups were neutral, while the amino group was protonated and positively charged in the solution. Under this condition, water solubility of linear F3 or F5 was thought to be improved, owing to the ionization of the *N*-terminus. On the other hand, NTA-conjugated ELPs possess no ionizable amino group at the *N*-terminus of the peptide due to elimination by the condensation reaction of NTA with F3 or F5. Therefore, the absence of *N*-terminal charge in the peptide was considered to be one of the causes for the increased hydrophobicity of these NTA-conjugated peptides. However, as NTA-conjugated ELPs have one basic nitrogen atom with a lone pair, the coacervation activity of these peptides could be affected by charge or hydration in acidic solutions. Therefore, it was considered necessary to examine the factors that could affect the hydrophobicity and charge of the peptide. For example, Ac-F5, an F5 analogue whose *N*-terminal amino group was simply acetylated, showed stronger coacervation ability than NTA-F5 (Figure S3). However, such peptide analogues that are simply acetylated at the *N*-terminal and possess no basic atom may not be sufficient as reference material toward NTA-conjugated analogues. NTA-2F3 and NTA-2F5 exhibited coacervation at concentrations 1 and 0.1 mg/mL, respectively (Figure 2C,E). In addition, NTA-2F5 exhibited higher coacervation ability than the F5-dimer (Cys-dimer), which was dimerized by a disulfide bond. The observation was congruent with a previous report.[22] By comparing the structures of the Cys-dimer and NTA-2F5, it was observed that the Cys-dimer possesses two ionizable amino groups, whereas NTA-2F5 has one ionizable carboxy group and one amino group derived from NTA. The difference in the number of functional groups that can be ionized under acidic conditions was thought to be one of the reasons for the obvious difference in self-assembling ability of the dimeric analogues. Under the conditions of nonionization, the coacervation abilities of NTA-2F5 and Cys-dimer were nearly identical (Figure S4). Notably, the concentrations for NTA-2F3 and NTA-2F5 were considerably lower than those of the corresponding monomers, F6 and F10 ($(FPGVG)_n$, $n = 6$ and 10), as reported previously.[52] In addition, NTA-3F3 showed coacervation at 0.1 mg/mL of concentration, whereas linear F9 required 1.0 mg/mL to show coacervation despite having the same number of amino acid residues (Figure S2). Therefore, we concluded that ELP multimerization was an efficient method to obtain thermoresponsive peptide analogues that exhibit LCST behavior even at low concentrations. Since NTA-3F5 was insoluble in water even at a concentration of 0.1 mg/mL, its coacervation ability could not be evaluated using the turbidity measurement method. The remarkable hydrophobic nature of NTA-3F5 owing to the relatively long peptide chain and the absence of free amino and

Table 2. T_t Values of NTA-Fn Analogues in Various Concentrations

peptide	concentration mg/mL	concentration mM	T_t (°C)[a]
F3	50	36.0	not determined
F5	40	17.4	23.7 ± 0.2
	30	13.0	32.8 ± 1.3
	20	8.67	47.8 ± 1.3
NTA-F3	50	32.0	18.7 ± 0.8
	40	25.6	24.0 ± 0.03
	30	19.2	31.9 ± 0.3
NTA-2F3	5.0	1.02	16.4 ± 0.3
	3.0	0.68	22.3 ± 0.3
	1.0	0.34	36.1 ± 0.1
NTA-3F3	0.50	0.12	13.8 ± 0.4
	0.30	0.07	16.7 ± 1.7
	0.10	0.02	35.9 ± 0.7
NTA-F5	7.0	2.83	19.3 ± 0.1
	5.0	2.02	25.9 ± 0.4
	3.0	1.21	42.7 ± 0.5
NTA-2F5	0.50	0.10	9.9 ± 0.3
	0.30	0.06	11.0 ± 0.7
	0.10	0.02	22.1 ± 0.9
NTA-3F5	0.10	0.01	not dissolved

[a]Data are shown with mean ± standard error. Each peptide was dissolved in pure water. The measurements were repeated at least three times.

https://dx.doi.org/10.1021/acsomega.0c06140
ACS Omega 2021, 6, 5705−5716

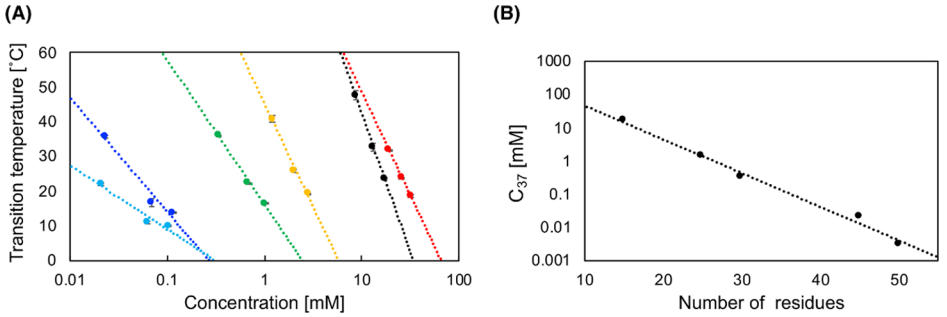

Figure 3. Correlation between T_t and peptide concentration of NTA-Fn analogues. (A) Relationships between the T_t and molar concentration of F5 (black line), NTA-F3 (red line), NTA-2F3 (green line), NTA-3F3 (blue line), NTA-F5 (yellow line), and NTA-2F3 (pale blue line). (B) Relationship between C_{37} and the number of residues of NTA-Fn analogues.

Table 3. Concentration Dependence of T_t of NTA-Conjugated ELPs

peptide	m	b	number of residues	M_w	C_{37} [mM]
F3	not determined	not determined	15	1389.62	not determined
F5	−34.86	122.85	25	2304.69	11.7
NTA-F3	−25.92	108.34	15	1562.75	15.7
NTA-2F3	−18.14	16.24	30	2934.36	0.31
NTA-3F3	−14.33	−18.84	45	4305.97	0.020
NTA-F5	−25.81	45.32	25	2477.81	1.38
NTA-2F5	−7.98	−9.30	50	4764.48	0.0030
NTA-3F5	not determined	not determined	75	7051.15	not determined

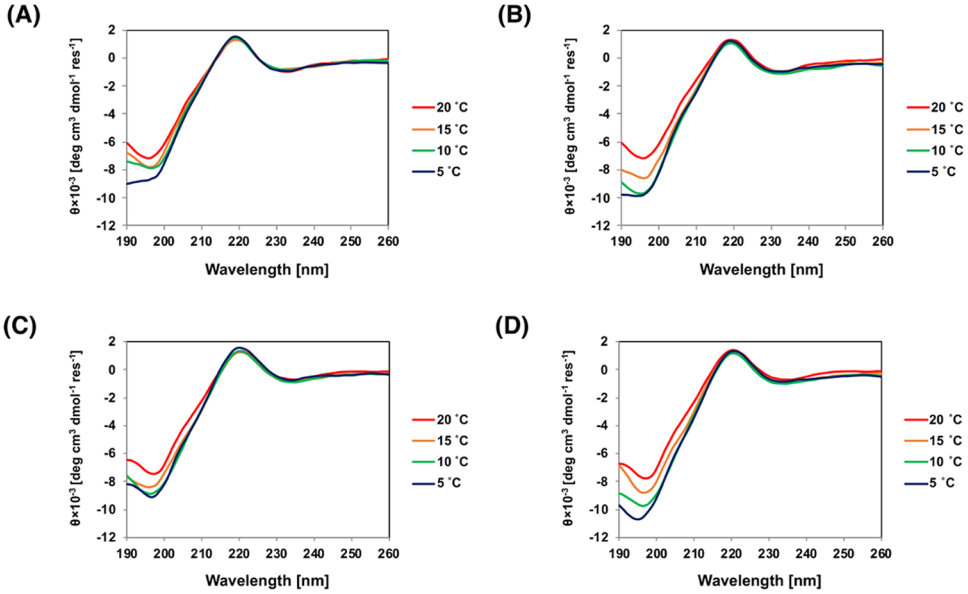

Figure 4. CD spectra of F3 and NTA-3F3 peptides. (A) F3 (heating), (B) F3 (cooling), (C) NTA-3F3 (heating), and (D) NTA-3F3 (cooling).

carboxy groups were thought to be responsible for the insolubility of NTA-3F5. Overall, NTA-conjugated $(FPGVG)_n$ analogues showed stronger coacervation activity than the corresponding linear counterparts that possessed the same numbers of amino acid residues. In addition, NTA-Fn analogues showed coacervation in pure water, whereas previous reports revealed that dendritic ELPs require relatively high concentration of kosmotropic salts such as sodium chloride (NaCl), which are typically used to salt out proteins from water, to exhibit coacervation in the aqueous solution.[35,39] These results suggest that multimerization of short ELPs via NTA is a powerful method to obtain ELP-like molecules exhibiting thermoresponsive property at low temperatures and concentrations.

The dependence of T_t on the peptide concentration was evaluated to compare the coacervation properties of the different NTA-Fn analogues. However, in this study, we were unable to directly compare the T_t value of synthesized peptide analogues at the same concentration, because the water solubility of these analogues was markedly different. Meyer and Chilkoti[16] demonstrated the relationship between T_t and the concentration of ELPs using the following equation

$$T_t = m \ln(C) + b \quad (1)$$

https://dx.doi.org/10.1021/acsomega.0c06140
ACS Omega 2021, 6, 5705−5716

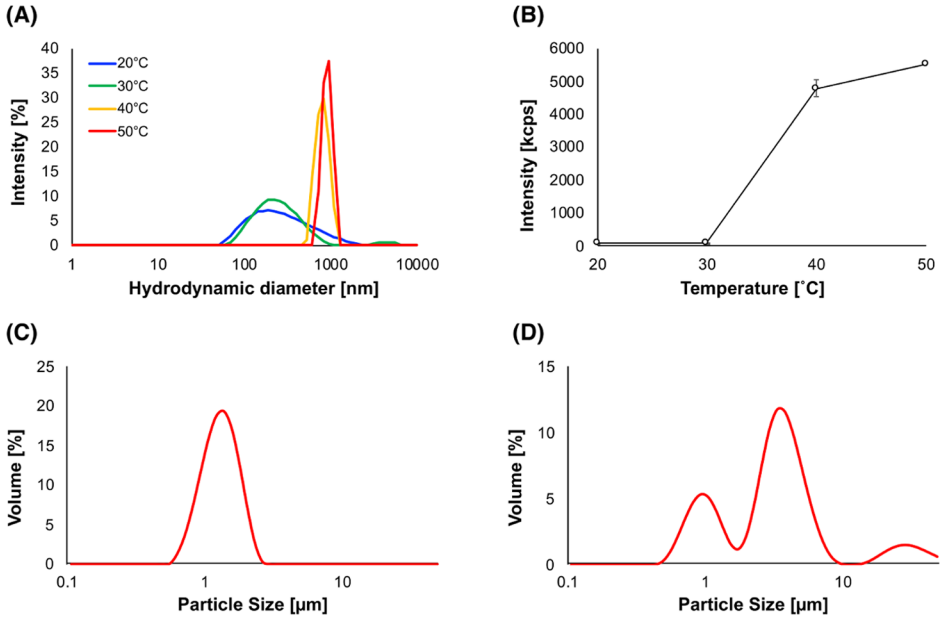

Figure 5. Particle size distribution of NTA-3F3 at various temperatures. (A) Size distribution of the coacervates and (B) temperature dependence of the average scattered intensity of the NTA-3F3 aqueous solution were analyzed by DLS measurements. In addition, the particle size distribution of NTA-3F3 aqueous solution after incubation at 50 °C for (C)10 min and (D) 3 h was analyzed by a laser diffraction particle size analyzer. The NTA-3F3 aqueous solution was prepared at a concentration of 0.10 mg/mL in pure water. Under this condition, the T_t value of NTA-3F3 was 35.9 °C.

The equation was used in this study to compare the self-assembling ability of each NTA-Fn analogue. T_t was plotted against the logarithm of the molar concentration of the peptide (Figure 3A). Similar to the linear $(FPGVG)_5$ analogue, the T_t of NTA-conjugated ELPs fitted well as the logarithmic functions of concentration. The proportionality constant (m) values of the synthesized peptides clearly decreased with dimerization and trimerization (Table 3). A similar trend was observed in NTA-F5 and NTA-2F5 as well. Therefore, it was suggested that the condensation of $(FPGVG)_n$ with NTA could change the concentration dependence of T_t. In addition, using this relationship, we calculated the C_{37} value, which is the concentration of the peptide used for each synthesized peptide analogue to attain T_t at 37 °C, by logarithmic extrapolation of the T_t vs peptide concentration graph (Table 3). Comparing these values, it was confirmed that NTA-3F3 and NTA-2F5 require very low concentrations for coacervation (C_{37} = 0.020 and 0.0030 mM, respectively) and showed very strong coacervation activity. In addition, the C_{37} values of NTA-conjugated ELP analogues decreased exponentially with increasing number of residues (Figure 3B). The results indicated conjugation and multimerization of ELPs with NTA to be one of the effective strategies for attaining improve coacervation ability. Furthermore, it was also confirmed that the quantitative relationship between C_{37} and the number of residues is useful to evaluate or estimate the coacervation activity of artificial NTA-conjugated short and nonlinear ELPs.

2.3. CD Measurement. CD spectra measurements of F3 and NTA-3F3 were carried out to investigate the influence of multimerization on the secondary structure of F3 (Figure 4). Comparison between Figure 4A,D revealed that the structural features of each peptide chain were not altered by trimerization. The spectra of F3 and NTA-3F3 showed almost the same characteristic bands: a minor negative band at 234 nm, a positive band at 220 nm, and a prominent negative band at 198 nm. These bands were also observed in the CD spectra of F5.[21] Furthermore, as temperature increased, the intensity of these three bands decreased. The change in the spectrum observed for both F3 and NTA-3F3 was reversible during the heating and cooling processes. These temperature-dependent changes in the bands were consistent with that of typical polyproline helix II (PPII) structures.[53,54] In addition, the positive band at 220 nm is another typical feature of the PPII structure.[55−57] The spectrum observed in the wavelength range of 230−260 nm was almost unchanged by temperature. On the other hand, the shoulder peak at 205 nm emerged with increasing temperature. These results indicated that the proportion of β-turn or β-sheet structure increases with rising temperature.[20] The results of CD measurement suggested that the temperature-dependent changes in the secondary structure of each peptide chain of the trimeric analogue were almost the same as that of the monomer and Cys-dimer, previously reported.[22] Therefore, multimerization of ELPs was supposed to enhance its coacervation ability without changing the secondary structural features.

2.4. Size Distribution of the Coacervates of NTA-3F3. To investigate the behavior of the coacervates arising from NTA-3F3 solutions, the size distribution of the coacervates was analyzed by dynamic light scattering (DLS) analysis at various temperatures, ranging from 20 to 50 °C. Figure 5A demonstrates the distribution of the peptide aggregates' hydrodynamic diameter. In this analysis, an NTA-3F3 peak was observed at approximately 200 nm between 20 and 30 °C. Thus, NTA-3F3 formed submicron aggregates at T_t, even though these aggregates did not show an apparent increase in turbidity. The size of the aggregates rapidly increased above T_t. At higher temperatures (40−50 °C), a larger hydrodynamic diameter (1−2 μm) of the particle was observed. In addition, the scattered light intensity of the NTA-3F3 solution was significantly increased above 40 °C. These results indicated that the micrometer-sized aggregates were formed at higher temperatures, above the LCST temperature. Even though the DLS

https://dx.doi.org/10.1021/acsomega.0c06140
ACS Omega 2021, 6, 5705−5716

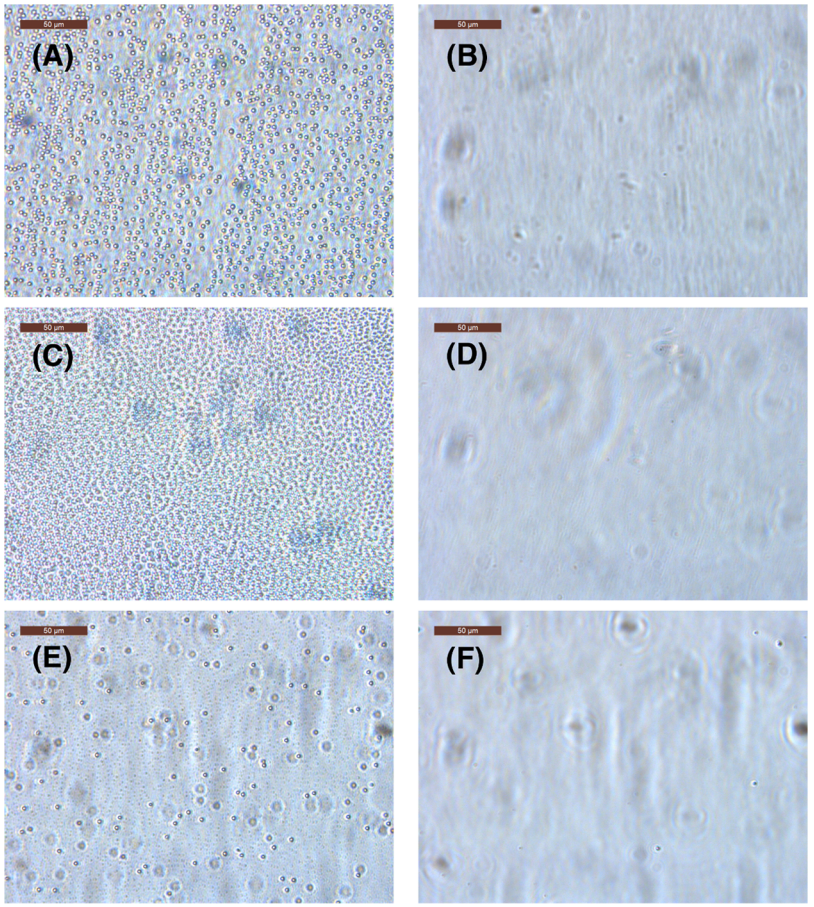

Figure 6. Optical microscopy images of NTA-F3 analogues. The images of (A) NTA-F3 (35 °C), (B) NTA-F3 (5 °C), (C) NTA-2F3 (20 °C), (D) NTA-2F3 (5 °C), (E) NTA-3F3 (17 °C), and (F) NTA-3F3 (5 °C) were obtained. Scale bars indicated 50 μm. The homogeneous aqueous solutions of each peptide were heated above T_t (A, C, and E) and then cooled to 5 °C (B, D, and F). NTA-3F3 was returned to homogeneous solution state by holding 5 °C for 15 min.

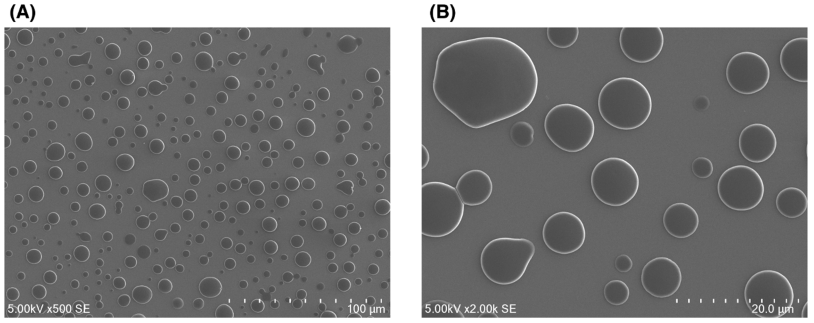

Figure 7. SEM image of self-assembled structure of NTA-3F3 coacervated at 50 °C. (A, B) 500× and 2000× magnification images, respectively. For preparation of the SEM sample, aqueous solution of 0.10 mg/mL NTA-3F3 was incubated at 50 °C for 3 h.

measuring instrument used in this study supported up to a size of 10 μm, the measurement results of NTA-3F3 particle size determined by DLS at a high temperature might be inaccurate, as particles > 1 μm may get deposited at the bottom of the measuring cuvette of DLS. To confirm the particle size distribution of coacervates at a temperature greater than T_t, particle size measurement at 50 °C was also carried out by laser diffraction particle size analysis. As shown in Figure 5C, NTA-3F3 formed aggregates of approximately 1.4 μm in diameter at 50 °C (average particle size was 1.40 ± 0.13 μm). This result was consistent with the DLS measurement. In addition, when the solution of NTA-3F3 was incubated at 50 °C for 3 h, larger particles (approximately 3.0 μm and 30 μm in diameter) were observed, implying that micrometer-sized coacervates grew together to form coacervates of several micrometers in diameter. Based on the particle size measurement analyses, it was suggested that the coacervation of NTA-3F3 probably follows a stepwise process involving generation of submicron aggregates followed by coacervate maturation. Such a stepwise process was also observed in a previous study on dendritic thermoresponsive ELP[34] and in a study wherein we reported strong coacervatable short ELPs.[23,24] According to previous studies relating to dendritic ELPs[34] or oligo (ethylene glycol) decorated dendrimers,[58,59] an aggregation state below T_t was presumed

https://dx.doi.org/10.1021/acsomega.0c06140
ACS Omega 2021, 6, 5705−5716

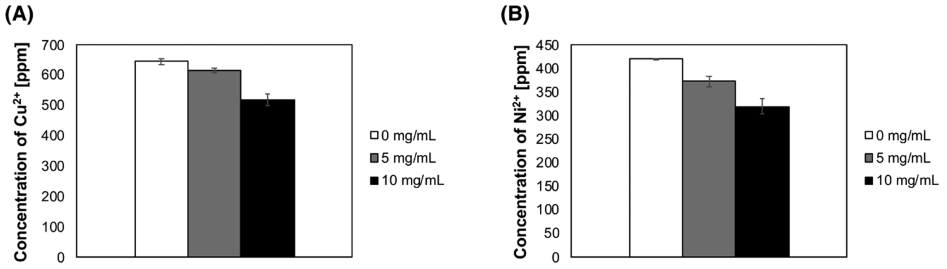

Figure 8. Metal-binding affinity of NTA-F5. $CuCl_2$ or $NiCl_2$ solution (10 mM) was treated with NTA-F5 at a concentration of 5.0 mg/mL (2.0 mM, gray bar) or 10 mg/mL (4.0 mM, black bar). The amount of (A) Cu^{2+} and (B) Ni^{2+} remained in supernatant solution phase was detected.

to be associated with the dehydration state of the molecule, which triggered the coacervation of ELPs. It was suggested that NTA-3F3 might undertake a secondary structure transition as a result of the dehydration-driven intra- and intermolecular hydrophobic interactions.

2.5. Morphology of Peptide Aggregates. The aggregates of NTA-Fn analogues were observed by optical microscopy to obtain the information on the morphology of the aggregates. The aggregates of NTA-nF3 in pure water are shown in Figure 6. All peptide aggregates were spherical and approximately 2−3 μm in diameter. NTA-F3 and NTA-2F3 formed aggregates above T_t (Figure 6A,C) and immediately dissociated and returned to its original solubilized state at 5 °C (Figure 6B,D). In contrast, NTA-3F3 formed more stable aggregates than NTA-F3 and NTA-2F3; cooling for approximately 15 min was required for NTA-3F3 to return to its original solution state (Figure 6F). Similar results were obtained for NTA-nF5 analogues (Figure S5). In particular, the aggregate of NTA-2F5 hardly returned to the original state even after being incubated at 5 °C overnight (Figure S5D). These results suggested that NTA-3F3 and NTA-2F5 formed stable coacervates and can be utilized as spherical base materials, for example as a DDS matrix and other biomaterials possessing controllable temperature-sensing properties. In addition, morphological analysis of the submicron coacervates of NTA-3F3 was carried out by scanning electron microscopy (SEM) as a preliminary study of the precise observation of aggregates (Figure 7). The spherical particles of diameter 1−20 μm, formed by aggregation of NTA-3F3, were observed. This result was comparable to the particle size measurements of laser diffraction particle size analysis after incubation at 50 °C for 3 h. On the other hand, for F5, spherical structures were not formed; instead, solids fixed in a paste-like manner were observed (Figure S6). This was probably because the concentration of the F5 solution used in the SEM sample preparation (0.1 mg/mL) was not sufficient to demonstrate aggregation. Utilizing formula (1), it was determined that a concentration of at least 8.09 mM (18.6 mg/mL) was required for F5 to show coacervation at 50 °C. These results showed that conjugation with NTA significantly enhances the coacervation ability of the $(FPGVG)_n$ analogue peptide and the NTA-$(FPGVG)_n$ peptides can form highly stable spherical peptide particles of several micrometers in diameter.

2.6. Evaluation of Affinity between NTA-F5 and Metal Ions. To investigate the interactions between NTA-Fn and metal ions, phase-transition behavior of NTA-F5 in the presence of NaCl, copper chloride ($CuCl_2$), and nickel chloride ($NiCl_2$) was evaluated. The results of the turbidity measurement and particle size distribution measurement by DLS were similar to that of pure water, although the T_t values of NTA-F5 increased in the solutions containing the three different salts (47.6 ± 0.5 °C in NaCl solution, 51.6 ± 1.4 °C in $CuCl_2$ solution, and 47.6 ± 0.3 °C in $NiCl_2$ solution) (Figure S7). The T_t value of NTA-F5 increased regardless of the metal salt being bound to NTA,[48] suggesting that the increment in T_t was probably caused by the salting-in effect of metal cations. The ability of salts to influence the solubility of proteins in aqueous solution is classified as the Hofmeister series.[60−62] Although the Hofmeister series for cations is less obvious than anions as the position of cation in the Hofmeister series could change in different phenomena,[62] it was reported that the divalent cations can increase the solubility of proteins or colloids.[62,63] Therefore, copper ion (Cu^{2+}) strongly enhanced the solubility of NTA-F5. However, the results of DLS measurement revealed that the self-assembling ability of NTA-F5 associated with temperature increment was retained. To evaluate whether the peptide can capture metal ions, colorimetric analysis was carried out using the aqueous solution of $CuCl_2$ in the presence or absence of NTA-F5. NTA-F5 and excess amount of $CuCl_2$ were dissolved in water and incubated at 50 °C to separate the coacervation and equilibrium solution phases. Then, the concentration of Cu^{2+} that remained in supernatant was detected by colorimetry. As shown in Figure 8A, the concentration of Cu^{2+} in $CuCl_2$ aqueous solution linearly decreased depending upon the concentration of NTA-F5. When NTA-F5 was added at a concentration of 10 mg/mL (4.0 mM), Cu^{2+} was reduced to 127.2 parts per million (ppm) (2.0 mM). According to this result, it was thought that Cu^{2+} and NTA-F5 forms a chelate in the ratio of 1:2. These results suggested that NTA-F5 can capture Cu^{2+} in a lower coacervation phase by forming a peptide-Cu^{2+} chelate. A similar measurement was also performed for nickel ion (Ni^{2+}) using the aqueous solution of $NiCl_2$ in the presence or absence of NTA-F5. To evaluate Ni^{2+} in the supernatant solution phase after treatment with NTA-F5, quantitative analysis was carried out using ICP-MS. As shown in Figure 8B, the concentration of Ni^{2+} in $NiCl_2$ aqueous solution also decreased depending upon the concentration of NTA-F5. However, compared to Cu^{2+}, decrease in the concentration of Ni^{2+} was slightly smaller. The results were consistent with previous studies that reported higher coordination of NTA with Cu^{2+} than with Ni^{2+}.[48] Hence, it was suggested that NTA-F5 could be also utilized as an easy-to-use metal scavenger with low environmental impacts.

3. CONCLUSIONS

In this study, novel ELP analogues with 1−3 molecules of $(FPGVG)_n$ (n = 3 or 5), NTA-Fn analogues, were synthesized to investigate the effect of multimerization on coacervation of ELPs, to control the self-assembly property of ELPs as novel biomaterials. Turbidity measurement demonstrated that multimerization via NTA significantly enhanced the coacervation

https://dx.doi.org/10.1021/acsomega.0c06140
ACS Omega 2021, 6, 5705−5716

ability of $(FPGVG)_n$ peptides. The C_{37} value, which is a concentration for each NTA-conjugated ELP analogue to attain T_t at 37 °C, showed an exponential decrease with increasing number of residues. Thus, C_{37} was suggested to be a useful parameter for evaluating or estimating the coacervation activity of NTA-conjugated short ELP analogues at body temperature. CD measurement revealed that the structure of NTA-3F3 exists as a PPII-like structure at lower temperatures and changes to a β-turn rich structure at higher temperatures, similar to the linear (FPGVG) peptide analogues and Cys-dimer. In conclusion, the study findings proposed that multimerization of short ELPs via NTA as core component is a useful strategy for obtain ELP-like molecules that exhibit thermoresponsive activity. Furthermore, results from microscopic studies indicated that NTA-3F3 and NTA-2F5 formed a very stable coacervate above the T_t, suggesting that these analogues can be utilized as useful base materials in DDS matrices that are suitable for targeted long-term drug delivery at body temperature. In addition, it was also revealed that NTA-Fn possessing only one peptide chain could capture metal ions such as Cu^{2+} or Ni^{2+} by the APCA component derived from NTA. The application of NTA-conjugated $(FPGVG)_n$ analogues as DDS carriers or metal-scavenging agents is currently under investigation.

4. EXPERIMENTAL SECTION

4.1. Chemicals. 9-Fluorenylmethyloxycarbonyl (Fmoc) amino acids were purchased from Merck Ltd. (Darmstadt, Germany). Fmoc-NH-SAL-MBHA resin (100−200 mesh), *N*,*N*-diisopropylethylamine (DIPEA), trifluoroacetic acid (TFA), and (1-cyano-2-ethoxy-2-oxoethylidenaminooxy) dimethylaminomorpholinocarbenium hexafluorophosphate (COMU) were purchased from Watanabe Chemical Industries Ltd. (Hiroshima, Japan). 2-(1*H*-benzotriazole-1-yl)-1,1,3,3-tetramethyl uronium hexafluorophosphate (HBTU) and 1-hydroxybenzotriazole (HOBt) were purchased from Kokusan Chemical Co., Ltd. (Tokyo, Japan). 1-Ethyl-3-(3-dimethylaminopropyl) carbodiimide monohydrochloride (WSCD) was purchased from Peptide Institute, Inc. (Osaka, Japan). Nitrilotriacetic acid (NTA), nitrilotriacetic acid disodium salt, 4-dimethylaminopyridine (DMAP), and triisopropylsilane (TIS) were purchased from Tokyo Chemical Industry Co., Ltd. (Tokyo, Japan). *N*,*N*-diethyldithiocarbamate (Na-DDTC) for quantification of copper ion was purchased from Nacalai Tesque Co. Ltd (Kyoto, Japan). Water for experiment was purified by Milli-Q Integral 3 (Merck Millipore, Darmstadt, Germany). Other solvents and reagents were also obtained from commercial suppliers and used without further purification.

4.2. Synthesis of $(FPGVG)_n$ Peptides. Elastin-derived peptide analogues H-$(FPGVG)_n$-NH_2 (n = 3 or 5, abbreviated as F3 or F5, respectively) were synthesized by an ABI 433A peptide synthesizer (Applied Biosystems, Foster City, CA) using the solid-phase method with Fmoc chemistry. HBTU (0.45 M) and HOBt (0.45 M) in *N*,*N*-dimethylformamide (DMF) were used as a condensing agent for peptide synthesis in FastMoc 0.25 mmol program included in SynthAssist 2.0 software (Applied Biosystems). After peptide chain extension, the peptide was cleaved from the resin with the reagents cocktail containing 95% TFA/2.5% TIS/2.5% H_2O. After cleavage, the resulting mixture was poured into 50 mL of diethyl ether and centrifuged to separate peptide precipitates from the cocktail. Then, the synthesized peptide analogues were prepurified using Sep-Pak Vac 35 cc C18 cartridge (Waters Co., Milford, MA) followed by final purification by high-performance liquid chromatography (HPLC). Purity and molecular weights of the peptides were confirmed by ACQUITY ultraperformance liquid chromatography (UPLC) H-Class (Waters Co.) equipped with an ACQUITY UPLC BEH C-18 column (100 mm; flow rate, 0.6 mL/min) (Waters Co.). Further detailed synthesis protocols are described in the Supporting Information.

4.3. Synthesis of NTA-Fn Analogues. NTA-Fn analogues were synthesized by conjugation between an *N*-terminal amino group of $(FPGVG)_n$ and a carboxyl group of NTA. Preparation of NTA-Fn and NTA-2Fn was performed with WSCD used as a condensing agent. H-$(FPGVG)_5$-NH_2 (142.9 mg, 0.062 mmol), NTA (3.82 mg, 0.014 mmol), 1-ethyl-3-(3-dimethylaminopropyl) carbodiimide monohydrochloride (water-soluble carbodiimide; WSCD, 23.7 mg, 0.12 mmol), 4-dimethyl-aminopyridine (DMAP, 1.22 mg, 0.01 mmol), and *N*,*N*-diisopropylethylamine (DIEPA, 42.4 μL, 0.24 mmol) were dissolved in a water/acetonitrile mixed solvent (3.8:1.2 mL, v/v) and stirred at 25 °C overnight to afford NTA-F5 and NTA-2F5 as a mixture. NTA-F3 and NTA-2F3 were synthesized in the same manner using 71.7 mg (0.052 mmol) of H-$(FPGVG)_3$-NH_2.To obtain NTA-3F5, H-$(FPGVG)_5$-NH_2 (57.8 mg, 0.025 mmol), NTA (1.31 mg, 0.00685 mmol), COMU (10.6 mg, 0.025 mmol), and DIEPA (3.59 μL, 0.021 mmol) were dissolved in 3 mL of DMF and stirred at 0 °C for 1 h. Then, the reaction mixture was warmed to 25 °C and stirred overnight to afford NTA-3F5. NTA-3F3 was synthesized in the same manner using 43.1 mg (0.031 mmol) of H-$(FPGVG)_3$-NH_2. Progress of the reaction was followed by UPLC-MS. After completion of the reaction, each peptide was prepurified using Sep-Pak Vac 35 cc C18 cartridge (Waters Co., Milford, MA) before final purification by HPLC. Each reaction mixture (including crude peptides) was applied to the Sep-Pak cartridge. Subsequently, eluent solution (mixed solvent of water/acetonitrile) was poured into the Sep-Pak cartridge. The concentration of acetonitrile in eluent was gradually increased to 15, 30, 40, 60, and 99% for peptide separation. The eluent solution was fractionated every 50 mL. Then, the eluent fraction containing peptide was identified by detecting UPLC-MS. The fraction was evaporated and lyophilized to obtain peptides as a colorless powder. Subsequently, further purification was performed by RP-HPLC (The Breeze 2 HPLC System, Waters Co.) equipped with a C8 column (COSMOSIL 5C8-AR-300 Packed Column, 20 mm I.D. × 150 mm, C8-AP 5 μm, 300 Å, Nacalai Tesque, Inc.) and a solvent system consisting of 0.1% TFA aqueous solution (v/v, solvent A) and a mixture of 80% acetonitrile and 20% solvent A (v/v, solvent B). The purified fraction was evaporated and lyophilized to obtain desired peptide analogues. The molecular weight and purity of the obtained peptide analogues were analyzed by UPLC-MS (Table 1 and Figure S1).

4.4. Turbidity Measurement. The temperature-dependent self-assembling property of the NTA-Fn analogues was evaluated using a JASCO V-660 spectral photometer (JASCO Co., Tokyo, Japan). Each peptide was dissolved in pure water at various concentrations. Turbidity was measured at 400 nm with increasing or decreasing temperature at a rate of 0.5 °C/min from 5 °C. Each concentration of sample solution was measured at least three times. Self-assembling property was described by the phase-transition temperature (T_t), which is the temperature at which the turbidity of the solution reaches half the maximum value.

4.5. CD Spectrum Measurement. CD measurement was carried out in a 1.0 mm path-length cuvette using a J-725 spectropolarimeter (JASCO Co.). Each peptide was dissolved in

https://dx.doi.org/10.1021/acsomega.0c06140
ACS Omega 2021, 6, 5705−5716

water at the concentration of 0.10 mg/mL. Measurements from 190 to 260 nm were performed at cell temperatures between 5 and 20 °C. For equilibration of the sample temperature, each measurement was performed after 5 min when the solution reached the target temperature. All spectra of sample peptides were obtained by subtracting the solvent spectra without peptide under the same conditions and smoothing with Savitzky−Golay smoothing filters.

4.6. Dynamic Light Scattering (DLS) Analysis. The distribution of the particle size in NTA-3F3 solution was analyzed by DLS measurement using Zetasizernano ZS (Malvern Instruments Ltd., Worcestershire, U.K.) in a measurement cell ZEN0112 (Malvern Instruments Ltd.). The NTA-3F3 aqueous solution was prepared at a concentration of 0.1 mg/mL in pure water and filtered using the Millex-LG filter (Merck Millipore) before measurement. DLS analysis was performed by increasing the temperature at 10 °C intervals from 20 to 50 °C. Measurement duration was selected automatically. Parameter dataset "protein" (dataset: refractive index, 1.450; absorption, 0.001) was used as the material parameter, and parameter dataset "water" (dataset: refractive index, 1.330; viscosity, 0.8872) was chosen as the dispersant parameter. Attenuation was selected automatically. The measurement of each concentration was performed at least three times.

4.7. Laser Diffraction Particle Size Measurement. The distribution of the particle size in NTA-3F3 solution over the transition temperature was analyzed by laser diffraction particle size measurement using Mastersizer 3000 (Malvern Instruments Ltd.). The NTA-3F3 aqueous solution was prepared at a concentration of 0.1 mg/mL in pure water. Then, 6.0 mL of the peptide solution was transferred to a batch cell. Before measurement, the peptide solution was incubated at 50 °C for 10 min or 3 h and then particle size measurement was carried out immediately. The measurement was performed three times.

4.8. Microscopic Study. The aggregates of NTA-Fn analogues were observed by microscopy using a Leica DM IL LED instrument (Leica Microsystems CMS GmbH, Wetzlar, Germany) equipped with an HI PLAN 40 × oil objective (Leica Microsystems CMS GmbH) and an HC PLAN 10 × eyepiece (Leica Microsystems CMS GmbH). The sample solutions were prepared in pure water at each concentration for 30 mg/mL NTA-F3, 3 mg/mL NTA-2F3, 0.3 mg/mL NTA-3F3, 3 mg/mL NTA-F5, and 0.3 mg/mL NTA-2F5. These samples (40 μL) were applied to a glass slide. Sample imaging was performed above T_t determined by the turbidity measurement and after cooling to 5 °C using Thermo Plate TP-CHSQM (Tokai Hit Co. Ltd., Shizuoka, Japan).

4.9. Scanning Electron Microscopy. Aqueous solution of 0.1 mg/mL NTA-3F3 was dropped on a cover glass and left at 50 °C for air drying. Subsequently, the residue was rinsed gently three times with distilled water and air-dried on the cover glass surface. The prepared sample was platinum sputter-coated (5 nm thick) and examined with an SU3500 (Hitachi High-Tech Corporation, Tokyo, Japan) at an operating voltage of 5.00 kV.

4.10. Colorimetric Analysis of Affinity of Copper Ions for NTA-F5. The colorimetric analysis of copper ions (Cu^{2+}) was carried out to evaluate the amount of copper ions absorbed into the coacervation phase of the NTA-F5 using a spectral photometer JASCO V-660 (JASCO Co.).[64] NTA-F5 was dissolved in 10 mM $CuCl_2$ aqueous solution (total 300 μL) at a concentration of 10 mg/mL (4.0 mM). The peptide solution was incubated at 50 °C for an hour to separate into a lower coacervation phase and an upper equilibrium solution phase. The supernatant of the equilibrium solution phase (10 μL) was added to 1 mL of 0.1% Na-DDTC solution. The resulting solution was extracted three times with 2 mL of ethyl acetate. Then, the combined organic layer was diluted to 10 mL with ethyl acetate. Subsequently, the concentration of copper ion (Cu^{2+}) was determined by measuring at 436 nm corresponding to the absorbance of yellow-brown complex $Cu(DDTC)_2$. The amount of copper ion absorbed in the peptide solution was determined by the calibration line. The measurement was performed at least three times.

4.11. Quantitative Analysis of the Affinity of Nickel Ions for NTA-F5 by ICP-MS. The quantitative analysis of nickel ions (Ni^{2+}) was carried out by ICP-MS to analyze the absorption amount of nickel ions into the coacervation phase of the NTA-F5 peptide. The quantitative analysis was performed using an Agilent Technologies 7500c inductively coupled plasma mass spectroscopy (ICP-MS) system (Agilent Technologies, Inc., Santa Clara, CA).[65] NTA-F5 was dissolved in 10 mM $NiCl_2$ aqueous solution at a concentration of 10 mg/mL (4.0 mM). The peptide solutions were incubated at 50 °C for an hour. After the incubation, the peptide solution was immediately centrifuged at room temperature for 1 min (6200 rpm) to remove aggregates. Then, 5 μL of supernatant of the equilibrium solution phase was diluted to 40 mL by pure water. The resulting solution was filtered by a syringe filter (pore size, 0.45 μm) (Sartorius, Goettingen, Germany). The concentration of nickel ions (Ni^{2+}) in the resulting solution was analyzed using ICP-MS. The amount of nickel ion absorbed in the peptide solution was determined by the calibration line. The measurement was performed at least three times.

■ ASSOCIATED CONTENT

Supporting Information

The Supporting Information is available free of charge at https://pubs.acs.org/doi/10.1021/acsomega.0c06140.

Detailed experimental procedure of the peptide synthesis, UPLC-MS analysis of NTA-Fn analogues (Figure S1); turbidity profiles of linear $(FPGVG)_n$ analogues (Figure S2); phase-transition profile of Ac-F5 (Figure S3); turbidity profiles of NTA-2F5 and Cys-dimer under nonionized conditions (Figure S4); optical microscopy images of NTA-F5 analogues (Figure S5); SEM image of F5 incubated at 50 °C (Figure S6); and turbidity change and particle size distribution of NTA-F5 in the presence of metal salts (Figure S7) (PDF)

■ AUTHOR INFORMATION

Corresponding Author

Takeru Nose − *Laboratory of Biomolecular Chemistry, Faculty of Arts and Science, Kyushu University, Fukuoka 819-0395, Japan; Department of Chemistry, Faculty and Graduate School of Science, Fukuoka 819-0395, Japan;* orcid.org/0000-0001-9771-7267; Phone: +81-92-802-6025; Email: nose@artsci.kyushu-u.ac.jp

Authors

Keitaro Suyama − *Laboratory of Biomolecular Chemistry, Faculty of Arts and Science, Kyushu University, Fukuoka 819-0395, Japan*

Mika Mawatari − *Department of Chemistry, Faculty and Graduate School of Science, Fukuoka 819-0395, Japan*

https://dx.doi.org/10.1021/acsomega.0c06140
ACS Omega 2021, 6, 5705−5716

Daiki Tatsubo − *Department of Chemistry, Faculty and Graduate School of Science, Fukuoka 819-0395, Japan*
Iori Maeda − *Department of Physics and Information Technology, Kyushu Institute of Technology, Fukuoka 820-8502, Japan*

Complete contact information is available at: https://pubs.acs.org/10.1021/acsomega.0c06140

Author Contributions

K.S. and M.M. carried out the experiment. K.S., M.M., D.T., and T.N. wrote the manuscript with support from all authors. I.M. helped supervise the project. K.S. and T.N. conceived the original idea. T.N. supervised the project.

Funding

This work was supported by JSPS KAKENHI Grant Number JP19H04303 and JP20K20638. The authors also thank E&C HealthCare Ltd. and ECC Co., Ltd. for financial support.

Notes

The authors declare no competing financial interest.

■ ACKNOWLEDGMENTS

The authors thank Dr. Midori Watanabe (Center of Advanced Instrumental Analysis, Kyushu University) for helping them during the SEM analysis. They also thank Editage (www.editage.com) for English language editing.

■ ABBREVIATIONS

APCA, aminopolycarboxylic acids; CD, circular dichroism; COMU, (1-cyano-2-ethoxy-3 oxoethylidenaminooxy) dimethylamino-morpholino-carbenium hexafluoro phosphate; DCM, dichloromethane; DDS, drug-delivery system; DDTC, diethyldithiocarbamate; DIPEA, *N*,*N*-diisopropylethylamine; DLS, dynamic light scattering; DMAP, 4-dimethyl-aminopyridine; DMF, *N*,*N*-dimethylformamide; ELP, elastin-like peptide; ESI, electrospray ionization; Fmoc, 9-fluorenylmethyloxycarbonyl; HBTU, 2-(1*H*-benzotriazole-1-yl)-1,1,3,3-tetramethyl uranium hexafluorophosphate; HOBt, 1-hydroxybenzotriazole; HPLC, high-performance liquid chromatography; ICP, inductively coupled plasma; LCST, lower critical solution temperature; MS, mass spectrum; NMP, *N*-methyl-2-pyrrolidone; NTA, nitrilotriacetic acid; PPII, polyproline helix II; SEM, scanning electron microscopy; TFA, trifluoroacetic acid; TIS, triisopropylsilane; T_t, phase-transition temperature; UPLC, ultrahigh-performance liquid chromatography; UV, ultraviolet; WSCD, 1-ethyl-3-(3-dimethylaminopropyl) carbodiimide monohydrochloride

■ REFERENCES

(1) Kim, Y. G.; Matsunaga, Y. T. Thermo-responsive polymers and their application as smart biomaterials. *J. Mater. Chem. B* **2017**, *5*, 4307−4321.
(2) McDaniel, J. R.; Callahan, D. J.; Chilkoti, A. Drug delivery to solid tumors by elastin-like polypeptides. *Adv. Drug Delivery Rev.* **2010**, *62*, 1456−1467.
(3) Rodríguez-Cabello, J. C.; Arias, F. J.; Rodrigo, M. A.; Girotti, A. Elastin-like polypeptides in drug delivery. *Adv. Drug Delivery Rev.* **2016**, *97*, 85−100.
(4) Fletcher, E. E.; Yan, D.; Kosiba, A. A.; Zhou, Y.; Shi, H. Biotechnological applications of elastin-like polypeptides and the inverse transition cycle in the pharmaceutical industry. *Protein Expression Purif.* **2019**, *153*, 114−120.
(5) Chen, J.; Zou, X. Self-assemble peptide biomaterials and their biomedical applications. *Bioact. Mater.* **2019**, *4*, 120−131.
(6) Chambre, L.; Martín-Moldes, Z.; Parker, R. N.; Kaplan, D. L. Bioengineered elastin- and silk-biomaterials for drug and gene delivery. *Adv. Drug Delivery Rev.* **2020**, *160*, 186−198.
(7) Chu, H. S.; Ryum, J.; Won, J.-I. Cadmium detection by a thermally responsive elastin copolymer with metal-binding functionality. *Enzyme Microb. Technol.* **2013**, *53*, 189−193.
(8) Choi, H.; Han, S.-J.; Won, J.-I. Thermal characteristics and cadmium binding behavior of EC-ELP fusion polypeptides. *Enzyme Microb. Technol.* **2020**, *140*, No. 109628.
(9) Zhao, M.; Rong, J.; Han, J.; Zhou, Y.; Li, C.; Wang, L.; Mao, Y.; Wang, Y. Novel Synthesis Strategy for Biocatalyst: Fast Purification and Immobilization of His- and ELP-Tagged Enzyme from Fermentation Broth. *ACS Appl. Mater. Interfaces* **2019**, *11*, 31878−31888.
(10) Mullerpatan, A.; Chandra, D.; Kane, E.; Karande, P.; Cramer, S. Purification of proteins using peptide-ELP based affinity precipitation. *J. Biotechnol.* **2020**, *309*, 59−67.
(11) Wang, S.; Lin, R.; Ren, Y.; Zhang, T.; Lu, H.; Wang, L.; Fan, D. Non-chromatographic purification of thermostable endoglucanase from Thermotoga maritima by fusion with a hydrophobic elastin-like polypeptide. *Protein Expression Purif.* **2020**, *173*, No. 105634.
(12) Vrhovski, B.; Weiss, A. S. Biochemistry of tropoelastin. *Eur. J. Biochem.* **1998**, *258*, 1−18.
(13) Yeo, G. C.; Keeley, F. W.; Weiss, A. S. Coacervation of tropoelastin. *Adv. Colloid Interface Sci.* **2011**, *167*, 94−103.
(14) Indik, Z.; Yeh, H.; Ornstein-Goldstein, N.; Sheppard, P.; Anderson, N.; Rosenbloom, J. C.; Peltonen, L.; Rosenbloom, J. Alternative splicing of human elastin mRNA indicated by sequence analysis of cloned genomic and complementary DNA. *Proc. Natl. Acad. Sci. U.S.A.* **1987**, *84*, 5680−5684.
(15) Raju, K.; Anwar, R. A. Primary structures of bovine elastin a, b, and c deduced from the sequences of cDNA clones. *J. Biol. Chem.* **1987**, *262*, 5755−5762.
(16) Bressan, G. M.; Argos, P.; Stanley, K. K. Repeating structure of chick tropoelastin revealed by complementary DNA cloning. *Biochemistry* **1987**, *26*, 1497−1503.
(17) Urry, D. W.; Long, M. M.; Cox, B. A.; Ohnishi, T.; Mitchell, L. W.; Jacobs, M. Synthetic polypentapeptide of elastin coacervates and forms filamentous aggregates. *Biochim. Biophys. Acta, Protein Struct.* **1974**, *371*, 597−602.
(18) Urry, D. W. Physical chemistry of biological free energy transduction as demonstrated by elastic protein-based polymers. *J. Phys. Chem. B* **1997**, *101*, 11007−11028.
(19) Maeda, I.; Taniguchi, S.; Ebina, J.; Watanabe, N.; Hattori, T.; Nose, T. Comparison between coacervation property and secondary structure of synthetic peptides, Ile-containing elastin-derived pentapeptide repeats. *Protein Pept. Lett.* **2013**, *20*, 905−910.
(20) Maeda, I.; Taniguchi, S.; Watanabe, N.; Inoue, A.; Yamasaki, Y.; Nose, T. Design of phenylalanine-containing elastin-derived peptides exhibiting highly potent self-assembling capability. *Protein Pept. Lett.* **2015**, *22*, 934−939.
(21) Taniguchi, S.; Watanabe, N.; Nose, T.; Maeda, I. Development of short and highly potent self-assembling elastin-derived pentapeptide repeats containing aromatic amino acid residues. *J. Pept. Sci.* **2016**, *22*, 36−42.
(22) Suyama, K.; Taniguchi, S.; Tatsubo, D.; Maeda, I.; Nose, T. Dimerization effects on coacervation property of an elastin-derived synthetic peptide $(FPGVG)_5$. *J. Pept. Sci.* **2016**, *22*, 236−243.
(23) Tatsubo, D.; Suyama, K.; Miyazaki, M.; Maeda, I.; Nose, T. Stepwise mechanism of temperature-dependent coacervation of the elastin-like peptide analog dimer, $(C(WPGVG)_3)_2$. *Biochemistry* **2018**, *57*, 1582−1590.
(24) Suyama, K.; Tatsubo, D.; Iwasaki, W.; Miyazaki, M.; Kiyota, Y.; Takahashi, I.; Maeda, I.; Nose, T. Enhancement of Self-Aggregation Properties of Linear Elastin-Derived Short Peptides by Simple Cyclization: Strong Self-Aggregation Properties of $Cyclo[FPGVG]_n$, Consisting Only of Natural Amino Acids. *Biomacromolecules* **2018**, *19*, 3201−3211.
(25) Keeley, F. W.; Bellingham, C. M.; Woodhouse, K. Elastin as a self-organizing biomaterial: use of recombinantly expressed human elastin

polypeptides as a model for investigations of structure and self-assembly of elastin. *Philos. Trans. R. Soc. London, Ser. B* **2002**, *357*, 185−189.
(26) Meyer, D. E.; Chilkoti, A. Quantification of the effects of chain length and concentration on the thermal behavior of elastin-like polypeptides. *Biomacromolecules* **2004**, *5*, 846−851.
(27) Girotti, A.; Reguera, J.; Arias, F. J.; Alonso, M.; Testera, A. M.; Rodríguez-Cabello, J. C. Influence of the Molecular Weight on the Inverse Temperature Transition of a Model Genetically Engineered Elastin-like pH-Responsive Polymer. *Macromolecules* **2004**, *37*, 3396−3400.
(28) McDaniel, J. R.; Radford, D. C.; Chilkoti, A. A unified model for de novo design of elastin-like polypeptides with tunable inverse transition temperatures. *Biomacromolecules* **2013**, *14*, 2866−2872.
(29) Kaibara, K.; Akinari, Y.; Okamoto, K.; Uemura, Y.; Yamamoto, S.; Kodama, H.; Kondo, M. Characteristic interaction of Ca^{2+} ions with elastin coacervate: ion transport study across coacervate layers of alpha-elastin and elastin model polypeptide, $(Val\text{-}Pro\text{-}Gly\text{-}Val\text{-}Gly)_n$. *Biopolymers* **1996**, *39*, 189−198.
(30) Maeda, I.; Fukumoto, Y.; Nose, T.; Shimohigashi, Y.; Nezu, T.; Terada, Y.; Kodama, H.; Kaibara, K.; Okamoto, K. Structural requirements essential for elastin coacervation: favorable spatial arrangements of valine ridges on the three-dimensional structure of elastin-derived polypeptide $(VPGVG)_n$. *J. Pept. Sci.* **2011**, *17*, 735−743.
(31) Iwanaga, A.; Endo, M.; Maeda, I.; Okamoto, K. Study on self assembly of pentapeptide repeating sequence in tropoelastin. *Pept. Sci. 2007* **2006**, 290−291.
(32) Urry, D. W.; Pattanaik, A. Elastic protein-based materials in tissue reconstruction. *Ann. N. Y. Acad. Sci.* **1997**, *831*, 32−46.
(33) Shmidov, Y.; Zhu, Y.; Matson, J. B.; Bitton, R. Effect of Crosslinker Topology on Enzymatic Degradation of Hydrogels. *Biomacromolecules* **2020**, *21*, 3279−3286.
(34) Shmidov, Y.; Zhou, M.; Yosefi, G.; Bitton, R.; Matson, J. B. Hydrogels composed of hyaluronic acid and dendritic ELPs: hierarchical structure and physical properties. *Soft Matter* **2019**, *15*, 917−925.
(35) Zhou, M.; Shmidov, Y.; Matson, J. B.; Bitton, R. Multi-scale characterization of thermoresponsive dendritic elastin-like peptides. *Colloids Surf., B* **2017**, *153*, 141−151.
(36) Navon, Y.; Zhou, M.; Matson, J. B.; Bitton, R. Dendritic Elastin-like Peptides: The Effect of Branching on Thermoresponsiveness. *Biomacromolecules* **2016**, *17*, 262−270.
(37) Ghoorchian, A.; Vandemark, K.; Freeman, K.; Kambow, S.; Holland, N. B.; Streletzky, K. A. Size and shape characterization of thermoreversible micelles of three-armed star elastin-like polypeptides. *J. Phys. Chem. B* **2013**, *117*, 8865−8874.
(38) Fukushima, D.; Sk, U. H.; Sakamoto, Y.; Nakase, I.; Kojima, C. Dual stimuli-sensitive dendrimers: Photothermogenic gold nanoparticle-loaded thermo-responsive elastin-mimetic dendrimers. *Colloids Surf., B* **2015**, *132*, 155−160.
(39) Kojima, C.; Irie, K.; Tada, T.; Tanaka, N. Temperature-sensitive elastin-mimetic dendrimers: Effect of peptide length and dendrimer generation to temperature sensitivity. *Biopolymers* **2014**, *101*, 603−612.
(40) Kojima, C.; Irie, K. Synthesis of temperature-dependent elastin-like peptide-modified dendrimer for drug delivery. *Biopolymers* **2013**, *100*, 714−721.
(41) Koga, T.; Iimura, M.; Higashi, N. Novel peptide-shelled dendrimer with dramatically changeable thermo-responsive character. *Macromol. Biosci.* **2012**, *12*, 1043−1047.
(42) Peppas, N. A.; Keys, K. B.; Torres-Lugo, M.; Lowman, A. M. Poly(ethylene glycol)-containing hydrogels in drug delivery. *J. Controlled Release* **1999**, *62*, 81−87.
(43) Bracci, L.; Falciani, C.; Lelli, B.; Lozzi, L.; Runci, Y.; Pini, A.; De Montis, M. G.; Tagliamonte, A.; Neri, P. Synthetic peptides in the form of dendrimers become resistant to protease activity. *J. Biol. Chem.* **2003**, *278*, 46590−46595.
(44) Aladini, F.; Araman, C.; Becker, C. F. W. Chemical synthesis and characterization of elastin-like polypeptides (ELPs) with variable guest residues. *J. Pept. Sci.* **2016**, *22*, 334−342.
(45) Ghoorchian, A.; Holland, N. B. Molecular architecture influences the thermally induced aggregation behavior of elastin-like polypeptides. *Biomacromolecules* **2011**, *12*, 4022−4029.
(46) Ghoorchian, A.; Cole, J. T.; Holland, N. B. Thermoreversible Micelle Formation Using a Three-Armed Star Elastin-like Polypeptide. *Macromolecule* **2010**, *43*, 4340−4345.
(47) Dhandhukia, J.; Weitzhandler, I.; Wang, W.; MacKay, J. A. Switchable elastin-like polypeptides that respond to chemical inducers of dimerization. *Biomacromolecules* **2013**, *14*, 976−985.
(48) Smith, R. M.; Martell, A. E. Critical stability constants, enthalpies and entropies for the formation of metal complexes of amino-polycarboxylic acids and carboxylic acids. *Sci. Total Environ.* **1987**, *64*, 125−147.
(49) Kostal, J.; Mulchandani, A.; Gropp, E. G.; Chen, W. A temperature responsive biopolymer for mercury remediation. *Environ. Sci. Technol.* **2003**, *37*, 4457−4462.
(50) Kostal, J.; Mulchandani, A.; Chen, W. Tunable biopolymers for heavy metal removal. *Macromolecules* **2001**, *34*, 2257−2261.
(51) Lao, U. L.; Chen, A.; Matsumoto, M. R.; Mulchandari, A.; Chen, W. Cadmium removal from contaminated soil by thermally responsive elastin (ELPEC20) biopolymers. *Biotechnol. Bioeng.* **2007**, *98*, 349−355.
(52) Maniwa, Y.; Inoue, A.; Watanebe, N.; Ogino, Y.; Yamasaki, Y.; Nose, T.; Maeda, I. Coacervation Properties of Hydrophobic Elastin-derived Pentapeptide Analogues. *Pept. Sci. 2013* **2012**, 391−392.
(53) Lopes, J. L.; Miles, A. J.; Whitmore, L.; Wallace, B. A. Distinct circular dichroism spectroscopic signatures of polyproline II and unordered secondary structures: applications in secondary structure analyses. *Protein Sci.* **2014**, *23*, 1765−1772.
(54) Lam, S. L.; Hsu, V. L. NMR identification of left-handed polyproline type II helices. *Biopolymers* **2003**, *69*, 270−281.
(55) Shi, Z.; Woody, R. W.; Kallenbach, N. R. Is polyproline II a major backbone conformation in unfolded proteins? *Adv. Protein Chem.* **2002**, *62*, 163−240.
(56) Shi, Z.; Olson, C. A.; Rose, G. D.; Baldwin, R. L.; Kallenbach, N. R. Polyproline II structure in a sequence of seven alanine residues. *Proc. Natl. Acad. Sci. U.S.A.* **2002**, *99*, 9190−9195.
(57) Bochicchio, B.; Tamburro, A. M. Polyproline II structure in proteins: identification by chiroptical spectroscopies, stability, and functions. *Chirality* **2002**, *14*, 782−792.
(58) Munkhbat, O.; Garzoni, M.; Raghupathi, K. R.; Pavan, G. M.; Thayumanavan, S. Role of aromatic interactions in temperature-sensitive amphiphilic supramolecular assemblies. *Langmuir* **2016**, *32*, 2874−2881.
(59) Fuller, J. M.; Raghupathi, K. R.; Ramireddy, R. R.; Subrahmanyam, A. V.; Yesilyurt, V.; Thayumanavan, S. Temperature-sensitive transitions below LCST inamphiphilic dendritic assemblies: host-guest implications. *J. Am. Chem. Soc.* **2013**, *135*, 8947−8954.
(60) Qiu, M.; Long, S.; Li, B.; Yan, L.; Xie, W.; Niu, Y.; Wang, X.; Guo, Q.; Xia, A. Toward an understanding of how the optical property of water-soluble cationic polythiophene derivative is altered by the addition of salts: The Hofmeister effect. *J. Phys. Chem. C* **2013**, *117*, 21870−21878.
(61) Rouster, P.; Pavlovic, M.; Szilagyi, I. Destabilization of titania nanosheet suspensions by inorganic salts: Hofmeister series and Schulze-Hardy rule. *J. Phys. Chem. B* **2017**, *121*, 6749−6758.
(62) Kang, B.; Tang, H.; Zhao, Z.; Song, S. Hofmeister Series: Insights of Ion Specificity from Amphiphilic Assembly and Interface Property. *ACS Omega* **2020**, *5*, 6229−6239.
(63) Tang, Y.; Li, H.; Zhu, H.; Tian, R.; Gao, X. Impact of electric field on Hofmeister effects in aggregation of negatively charged colloidal minerals. *J. Chem. Sci.* **2016**, *128*, 141−151.
(64) Jankiewicz, B.; Ptaszynski, B.; Turek, A. Spectrophotometric determination of cooper(II) in samples of solid from selected allotment gardens in Lodz. *Pol. J. Environ. Stud.* **1999**, *8*, 35−38.
(65) Chen, H.; Dabek-Zlotorzynska, E.; Rasmussen, P. E.; Hassan, N.; Lanouette, M. Evaluation of semiquantitative analysis mode in ICP-MS. *Talanta* **2008**, *74*, 1547−1555.

https://dx.doi.org/10.1021/acsomega.0c06140
ACS Omega 2021, 6, 5705−5716